sufficed. However, for smaller frequency spacings multiuser detection is required, yielding near-single-user performance in the case $\Delta fT = 1/2$, $\Delta\varphi = \pi/2$. (With $\Delta fT = 1/2$, $\Delta\varphi = 0$, the composite signal constellation is smaller than m^K owing to identical signals.)

In Fig. 3, we study the dependency on K for $\Delta fT = 1/2$, $\Delta\varphi = \pi/2$ and $\Delta fT = 1/3$, $\Delta\varphi = 0$. In the former case, the loss is negligible at BER = 10^{-3} for $K = 5$ compared to $K = 1$. Finally, Fig. 4 shows results for $K = 2$, 3 and 5 in the CDMA (cochannel interference) case $\Delta fT = 0$. It is seen that performance depends strongly on the relative phases between the users. A proper choice, e.g. $\Delta\varphi = \pi/2$ for $K = 3$, can give a power/bandwidth efficiency of 2.2 dB/0.8 [Note 1] which is better than for any previously known SCCPM system.

Conclusions: Multiuser SCCPM with a high degree of spectral overlap has been investigated using an iterative decoder. Simulation results indicate that for frequency spacings of at least one-third the CPM symbol rate, up to five equal-power users can be detected with a loss of no more than 1.4 dB compared to the single-user case. In addition, with no frequency spacing at all, three users can be detected with a loss of only 0.8 dB, but this is strongly dependent on the relative phases between the users.

Acknowledgments: This work was supported by Ericsson Mobile Data Design AB, Sweden, and the Foundation for Strategic Research through a Senior Individual Grant.

4 July 2001
Electronics Letters Online No: 20010807
DOI: 10.1049/el:20010807

P. Moqvist and T. Aulin (*Department of Computer Engineering, Chalmers University of Technology, SE-412 96 Göteborg, Sweden*)

E-mail: pmoqvist@ce.chalmers.se

References

1 MOQVIST, P.: 'Serially concatenated systems: an iterative decoding approach with application to continuous phase modulation'. Lic.Eng. thesis, Department of Computer Engineering, Chalmers University of Technology, Göteborg, Sweden, 1999. Also available at http://www.ce.chalmers.se/TCT

2 NARAYANAN, K.R., and STÜBER, G.L.: 'Performance of trellis coded CPM with iterative demodulation and decoding'. Proc. IEEE Global Telecommun. Conf., Rio de Janeiro, Brazil, Dec. 1999, pp. 2346–2351

3 MOHER, M.: 'An iterative multiuser decoder for near-capacity communications', *IEEE Trans. Commun.*, 1998, **46**, (7), pp. 870–880

4 REED, M.C., SCHLEGEL, C.B., ALEXANDER, P.D., and ASENSTORFER, J.A.: 'Iterative multiuser detection for CDMA with FEC: near-single-user performance', *IEEE Trans. Commun.*, 1998, **46**, (12), pp. 1693–1699

5 BENEDETTO, S., MONTORSI, G., DIVSALAR, D., and POLLARA, F.: 'Soft-input soft-output modules for the construction and distributed iterative decoding of code networks', *Eur. Trans. Telecommun.*, 1998, **9**, (2), pp. 155–172

Shortest path routing algorithm using Hopfield neural network

C.W. Ahn, R.S. Ramakrishna, C.G. Kang and I.C. Choi

A near-optimal routing algorithm employing a modified Hopfield neural network (HNN) is presented. Since it uses every piece of information that is available at the peripheral neurons, in addition to the highly correlated information that is available at the local neuron, faster convergence and better route optimality is achieved than with existing algorithms that employ the HNN. Furthermore, all the results are relatively independent of network topology for almost all source-destination pairs.

Note 1: Power efficiency measured as required E_k^b/N_0 for BER = 10^{-3}; bandwidth efficiency measured as double-sided 99% bandwidth normalised to the composite source bit rate.

Introduction: Hopfield and Tank [1] initially demonstrated the computational power of the neural network (NN) by applying their models to the travelling salesman problem (TSP). The advantage of the Hopfield neural network (HNN) is the hardware-based rapid computational capability of solving the combinatorial optimisation problem. Subsequently, the shortest path (SP) routing problem was addressed using the HNN under various constraints. In particular, Ali and Kamoun [2] proposed an adaptive algorithm that utilised link cost and topology information. However, the computed paths in this algorithm involved loops, and convergence could be slow. Invoking additional constraint on the flow vector, Park and Choi [3] proposed a modified algorithm. This enhanced the convergence performance, which, however, was heavily dependent on the network topologies. In this Letter, a new approach is proposed to speed up convergence while improving route optimality, and which is relatively insensitive to variations in network topology.

Proposed approach: A network topology can be described by the undirected graph $\mathbf{G} = (\mathbf{N}, \mathbf{A})$, where $\mathbf{N}$ is a set of N nodes (vertices) and $\mathbf{A}$ is a set of links (arcs or edges) [1 – 3]. The link connection indicator ρ_{ij} is defined as follows:

$$\rho_{ij} = \begin{cases} 1 & \text{if link from node } i \text{ to node } j \text{ does not exist} \\ 0 & \text{otherwise} \end{cases}$$

There is a cost C_{ij} associated with each link (i, j) and they are specified by the cost matrix $\mathbf{C} = [C_{ij}]$. Source and destination nodes are denoted by s and d, respectively. A path inclusion criterion matrix, denoted by $\mathbf{V} = [V_{ij}]$, represents the output values of neurons and each element is defined as follows:

$$V_{ij} = \begin{cases} 1 & \text{if link from node } i \text{ to node } j \text{ exists in routing path} \\ 0 & \text{otherwise} \end{cases}$$

It is obvious that all the diagonal elements of V_{ij} must be zero. Using the above definitions, the SP problem can be formulated as a constrained combinatorial optimisation problem:

$$\text{minimise} \quad \sum_{i=1}^{N}\sum_{\substack{j=1\\ j\neq i}}^{N} C_{ij}\cdot V_{ij}$$

$$\text{subject to} \quad \sum_{\substack{j=1\\ j\neq i}}^{N} V_{ij} - \sum_{\substack{j=1\\ j\neq i}}^{N} V_{ji} = \begin{cases} 1 & \text{if } i = s \\ -1 & \text{if } i = d \\ 0 & \text{otherwise} \end{cases}$$

$$V_{ij} \in \{0, 1\} \qquad (1)$$

The constraint, eqn. 1, ensures that the computed result is indeed a path between a source and a designated destination. To formulate this optimisation problem in terms of the HNN, the computational network requires $N(N-1)$ neurons since it is organised in an $(N \times N)$ matrix with all diagonal elements removed. Defining the Lyapunov (energy) function as eqn. 2, its minimisation drives each neuron of the NN into its stable state, thereby providing the SP solution:

$$E = \frac{\mu_1}{2}\sum_{i=1}^{N}\sum_{\substack{j=1\\ j\neq i}}^{N} C_{ij}\cdot V_{ij} + \frac{\mu_2}{2}\sum_{i=1}^{N}\sum_{\substack{j=1\\ j\neq i}}^{N}\rho_{ij}\cdot V_{ij}$$
$$+ \frac{\mu_3}{2}\sum_{i=1}^{N}\left(\sum_{\substack{j=1\\ j\neq i}}^{N} V_{ij} - \sum_{\substack{j=1\\ j\neq i}}^{N} V_{ji} - \gamma_i\right)^2 + \frac{\mu_4}{2}\sum_{i=1}^{N}\sum_{\substack{j=1\\ j\neq i}}^{N} V_{ij}\cdot(1 - V_{ij})$$
$$+ \frac{\mu_5}{2}\sum_{i=1}^{N}\sum_{\substack{j=1\\ j\neq i}}^{N} V_{ij}\cdot V_{ji} + \frac{\mu_6}{2}\left[\sum_{i=1}^{N}\sum_{\substack{j=1\\ j\neq i}}^{N}\left(\sum_{\substack{k=1\\ k\neq i,j}}^{N} V_{ik} - 1\right)\cdot V_{ij}^2\right]$$
$$+ \frac{\mu_7}{2}\left[\sum_{i=1}^{N}\sum_{\substack{j=1\\ j\neq i}}^{N}\left(\sum_{\substack{k=1\\ k\neq i,j}}^{N} V_{kj} - 1\right)\cdot V_{ij}^2\right] \qquad (2)$$

where

$$\gamma_i = \begin{cases} 1 & \text{if } i = s \\ -1 & \text{if } i = d \\ 0 & \text{if } i \neq s, d \end{cases}$$

and $\{\mu_i\}$ are the constants. In eqn. 2, the μ_1 term minimises the

total link cost of a routing path by taking into account the cost of all existing links; the μ_2 term prevents non-existent links from being included in the chosen routing path; the μ_3 term oversees constraint (eqn. 1) satisfaction and maintains the equality of the number of incoming and outgoing links; the μ_4 term drives the neurons towards convergence to a valid route consisting of connected nodes. The above four terms were included by Ali and Kamoun in their original formulation [2]. To guarantee that the flow vector is always directed towards the destination, i.e. not to include the reverse link in the route once the corresponding forward link is included in that, the μ_5 term was proposed by Park and Choi [3]. The μ_6 and μ_7 terms are being added by the present authors to eliminate the possibility of loops or partitions in a path. These terms also nudge the neurons towards speedy and precise convergence to an optimal solution.

The proposed HNN uses all the information available at the peripheral neurons. Furthermore, it draws on the highly correlated knowledge at the local neuron. In fact, the proposed algorithm strives to employ every piece of information available with the neuron, which counters a tendency to converge to one of the sub-optimal paths reachable with only the local information. Thus the corresponding modification allows for speedy and optimal convergence.

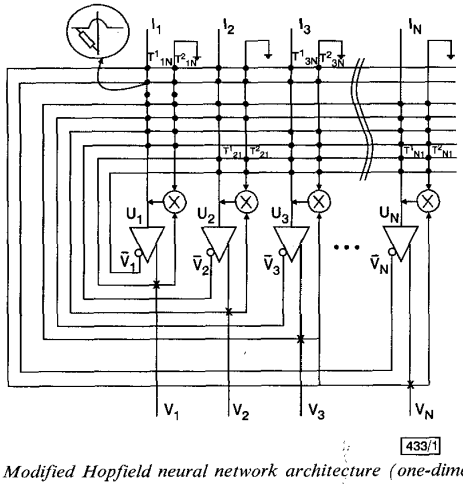

Fig. 1 *Modified Hopfield neural network architecture (one-dimensional case)*

Modifying the conventional HNN so as to derive the aforementioned benefit, the resulting architecture follows (as illustrated in Fig. 1 for the one-dimensional case) and the dynamics of HNN are described by eqn. 3, i.e.

$$\frac{dU_{ij}}{dt} = -\frac{U_{ij}}{\tau} + \sum_{k=1}^{N}\sum_{\substack{l=1 \\ l\neq k}}^{N}\left\{T^{(1)}_{ij,kl}V_{kl} + T^{(2)}_{ij,kl}V_{kl}V_{ij}\right\} + I_{ij} \tag{3}$$

where τ is the time constant of the circuit. The dynamics of the neuron at link (i, j) is described by eqn. 4, i.e.

$$\frac{dU_{ij}}{dt} = -\frac{U_{ij}}{\tau} - \frac{\partial E}{\partial V_{ij}} \tag{4}$$

Equating eqn. 3 with eqn. 4 subject to eqn. 2, the connection strength and bias are found to be

$$T^{(1)}_{ij,kl} = \mu_3\delta_{jk} + \mu_3\delta_{li} - \mu_3\delta_{ik} - \mu_3\delta_{jl} + \mu_4\delta_{ik}\delta_{jl} - \frac{\mu_5}{2}\delta_{jk}\delta_{il} - \mu_6\delta_{ik}\delta_{jl} - \mu_7\delta_{ik}\delta_{jl} \tag{5}$$

$$T^{(2)}_{ij,kl} = -\mu_6\delta_{ik} - \mu_7\delta_{jl} \tag{6}$$

$$I_{ij} = -\frac{\mu_1}{2}C_{ij} - \frac{\mu_2}{2}\rho_{ij} + \mu_3\gamma_i - \mu_3\gamma_j - \frac{\mu_4}{2} \tag{7}$$

where δ_{ij} is the Kronecker delta function. The HNN finds the SP between any two nodes by properly adjusting the input biases in eqn. 7.

Simulation results and discussion: Computer simulation is used to compare the performance of the proposed algorithm with those of Ali and Kamoun [2] and Park and Choi [3] for a 14-node example network. Fig. 2 compares the route costs achieved by the algorithms, in which Dijkstra's algorithm provides a reference of optimal result. Clearly, the proposed algorithm exhibits fastest convergence; indeed, it converges to a value that is close to Dijkstra's optimal cost, notwithstanding the inherent initial disadvantage. The anomaly of total route cost, which drops below Dijkstra's optimal cost in the course of iterations, may be explained by the fact that Dijkstra's algorithm employs discrete computation while other approaches work with continuous values.

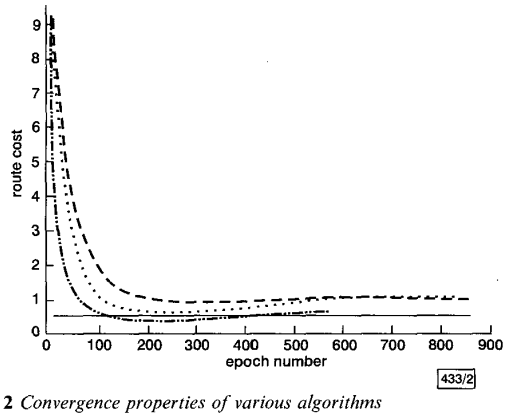

Fig. 2 *Convergence properties of various algorithms*

——— Dijkstra algorithm
- - - - Ali and Kamoun [2]
····· Park and Choi [3]
— ·· — proposed

Table 1: Performance comparison

Performance measure		Algorithm		
		Ali and Kamoun [2]	Park [3]	Proposed
Number of iterations	Average	505.67	504.79	399.69
	Standard deviation	256.75	283.63	232.74
Route optimality, %		86.52	85.96	93.82

A total of 10000 random network topologies with varying sizes and randomly assigned (normalised) link costs were investigated. Table 1 compares the algorithms. The proposed algorithm converges to a stable state in about 400 iterations, about 20% improvement over the algorithms in [2, 3]. Furthermore, it attains about 94% of route optimality performance, about 7 to 8% improvement over those algorithms. In Table 1, the route optimality refers to the percentage of the correct optimal routes found by the proposed approach in the random network topologies tested in the experiment.

Conclusion: The proposed algorithm results in speedy convergence to a stable state while improving route optimality. Its performance is relatively insensitive to variations in network topology. Hardware implementation of the HNN architecture modified with the current proposal can be useful for solving the shortest path routing problems in the rapidly varying network topology as in the emerging mobile *ad hoc* networks.

25 June 2001
Electronics Letters Online No: 20010800
DOI: 10.1049/el:20010800

C.W. Ahn and R.S. Ramakrishna (*Department of Information & Communications, Kwang-Ju Institute of Science and Technology, Oryong-dong 1, Puk-gu, Kwang-Ju 500-712, Korea*)

C.G. Kang (*School of Electrical Engineering, Korea University, 5-1 Ka, Anam-dong, Sungbuk-ku, Seoul 136-701, Korea*)

I.C. Choi (*Department of Industrial Systems and Information Engineering, Korea University, 5-1 Ka, Anam-dong, Sungbuk-ku, Seoul 136-701, Korea*)

References

1 HOPFIELD, J.J., and TANK, D.W.: 'Neural computations of decisions in optimization problems', *Biol. Cybern.*, 1986, **52**, pp. 141–152

2 ALI, M.K.M., and KAMOUN, F.: 'Neural networks for shortest path computation and routing in computer networks', *IEEE Trans. Neural Netw.*, 1993, **4**, (6), pp. 941–954
3 PARK, D.C., and CHOI, S.E.: 'A neural network based multi-destination routing algorithm for conmumcation network'. Proc. Jnt. Conf. Neural Networks, Anchorage, USA, 1998, pp. 1673–1678

84 fs PMD detection sensitivity in 2 × 40 Gbit/s RZ polarisation multiplex transmission experiment

D. Sandel, R. Noé, V. Mirvoda, S. Hinz and F. Wüst

Interchannel phase modulation of polarisation-multiplexed optical signals results in pulse arrival time variations in the presence of polarisation mode dispersion (PMD). Integration of the voltage controlled oscillator (VCO) input signal in the clock recovery phase locked loop (PLL) allows detection of these. 150 and 84 fs PMD detection sensitivities are demonstrated for 4.8 and 38.4 μs measurement intervals, respectively.

Introduction: Polarisation division multiplex (PolDM) transmission of two data signals on one optical carrier is attractive to double fibre capacity [1]. Return-to-zero (RZ) PolDM transmission has also been demonstrated [2]. Interchannel interference, tailored by interchannel phase modulation, was detected to correct polarisation mismatch at the receiver. In this Letter, we show that this modulation also allows detection of polarisation mode dispersion (PMD) because it varies the pulse arrival times. The resulting PMD detection sensitivity is better than for any other reported scheme [3 – 6], at least one order of magnitude when expressed in fractions of the pulse duration. This is because the error signal is proportional to this quotient, and not just to its square.

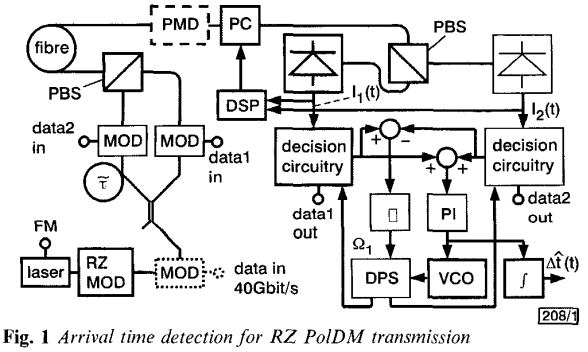

Fig. 1 *Arrival time detection for RZ PolDM transmission*

Theory: We consider the RZ data format which is generally preferred over the NRZ format owing to its better nonlinearity tolerance. Assume the two bit streams are transmitted simultaneously (without interchannel time delay) with $\pm S_1$ polarisations after combination in a polarisation beamsplitter (PBS) (Fig. 1). A small sinusoidal FM applied to the transmitter laser in conjunction with an interchannel time delay $\tilde{\tau}$ before one of the data modulators (MOD) modulates the interchannel phase difference [2]. Another PBS demultiplexes the signals in the receiver. A signal processor (DSP) monitors detected interchannel interference terms and minimises them by appropriate setting of a polarisation controller (PC). At the same time it assures that any PMD vector component τ_1 between the two transmitted signals results in only a static time delay between the two received bit streams. This can be taken care of by two individual clock recoveries (this possibility is not shown) or a differential clock phase shifter (DPS) that may be controlled by the integral of the measured clock phase differences in the two receiver branches. The other, detrimental PMD vector components τ_2, τ_3 can also be detected: the interchannel phase difference causes a common mode arrival time modulation $\Delta\hat{t}(t)$ of the RZ PolDM signals, which has to be absorbed by the clock recovery PLL. Integration of the VCO input signal allows recovery of $\Delta\hat{t}(t)$. The RMS amplitude of a suitable linear combination of at least one even and at least one odd line of the resulting Bessel spectrum [2] is proportional to $\Delta\hat{t}_{rms} = 2^{-3/2}\sqrt{(\tau_2^2 + \tau_3^2)}$.

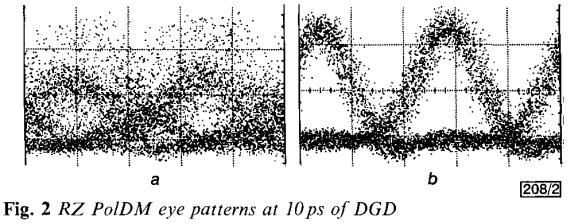

Fig. 2 *RZ PolDM eye patterns at 10 ps of DGD*

a Worst case
b Best case

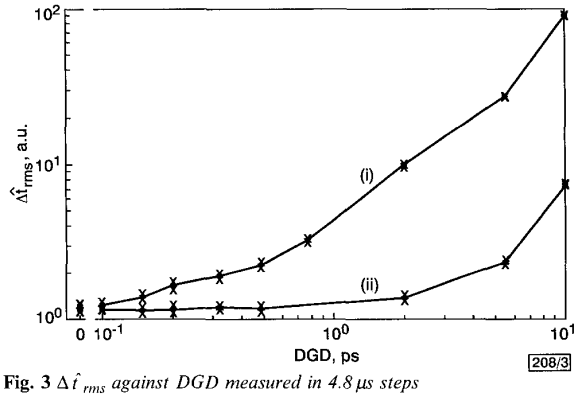

Fig. 3 $\Delta\hat{t}_{rms}$ *against DGD measured in 4.8 μs steps*

Zero DGD point separated from logarithmic axis
(i) worst case
(ii) best case

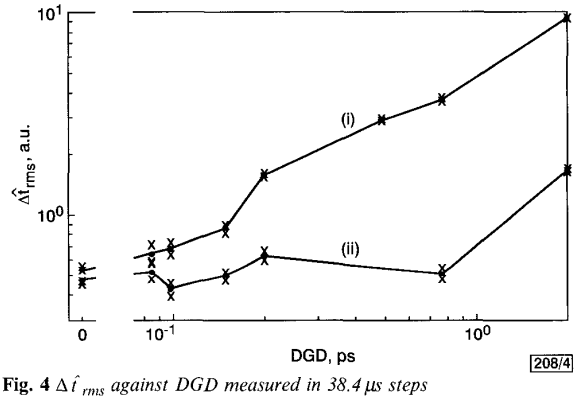

Fig. 4 $\Delta\hat{t}_{rms}$ *against DGD measured in 38.4 μs steps*

Zero DGD point separated from logarithmic axis
(i) worst case
(ii) best case

Experiment: A 2 × 40 Gbit/s RZ PolDM transmission system was set up, with improved clock recovery. A 417 kHz FM was applied to the TX laser to generate interchannel phase modulation with an index $\eta = 4.2$. A Mach-Zehnder modulator (RZ MOD) driven at 20 GHz generated a 400 Hz RZ pulse stream. For simplicity, a common data modulator (Fig. 1, dotted MOD) was placed in front of the polarisation multiplexer, and all shaded components were left out. In the receiver an $LiNbO_3$ device served as a PC. A linear combination of Bessel lines 2, 3 and 4 in the photocurrent was detected and minimised by DSP/PC. Similar processing of $\Delta\hat{t}(t)$ allowed determination of $\Delta\hat{t}_{rms}$ simultaneously. The VCO was connected directly to the decision circuitry without DPS. For each DGD the polarisations at the input of a PMD test module were adjusted for maximum $\Delta\hat{t}_{rms}$ ($\tau_1 = 0$, $\sqrt{(\tau_2^2 + \tau_3^2)}$ = max.) as the worst case (Fig. 2*a*, and top traces in Figs. 3 and 4), and for most DGDs also at minimum $\Delta\hat{t}_{rms}$ ($|\tau_1|$ = max., $\sqrt{(\tau_2^2 + \tau_3^2)} = 0$) as the best case (Fig. 2*b*, and bottom traces in Figs. 3 and 4). The sensitivity limit, defined by non-overlapping $\pm 1 - \sigma$ error intervals (× symbols), was 150 fs (Fig. 3) and 84 fs (Fig. 4) for 4.8 and 38.4 μs-long measurement intervals, respectively. The latter DGD